Water Practice & Technology

IWA PUBLISHING

Water Practice & Technology Vol 18 No 6, 1479 doi: 10.2166/wpt.2023.086

Removal of ammonia nitrogen from wastewater using activated carbon prepared from waste tyres

John Kabuba * and Joseph Lephallo

Department of Chemical and Metallurgical Engineering, Faculty of Engineering and Technology, Vaal University of Technology, Private Bag X021, Vanderbijlpark, South Africa
*Corresponding author. E-mail: johnka@vut.ac.za

JK, 0000-0002-0099-6245

ABSTRACT

In this work, the removal of ammonia nitrogen (NH_4-N) on activated carbon prepared from waste tyres was conducted in batch studies as a function of adsorbent dosage, pH, temperature, contact time and initial concentration. The pore structure of activated carbon was characterized by N_2 adsorption. The optimal conditions for the efficient adsorption of ammonia nitrogen onto waste tyre-activated carbon were found to be an adsorbent dosage of 0.4 g/L, pH 9.0, temperature of 20 °C, contact time of 90 min and initial ammonium nitrogen concentration of 50 mg/L. The kinetics studies showed that the pseudo-second-order model offered the best connection of the adsorption data. The Langmuir model was found to provide the best fit for the experimental data. The thermodynamic results showed that the adsorption of ammonia onto waste tyre-activated carbon was exothermic, random and spontaneous in nature.

Key words: activated carbon, adsorption, ammonia nitrogen, waste tyre, wastewater

HIGHLIGHTS

- Ammonia nitrogen was removed from wastewater using activated carbon prepared from waste tyres.
- Pore structure of activated carbon was characterized by N_2 adsorption.
- Optimal conditions for efficient adsorption were found as follows: an adsorbent dosage of 0.4 g/L, pH 9.0, temperature of 20 °C, contact time of 90 min and initial concentration of 50 mg/L.
- The adsorption process, isotherms, kinetic and thermodynamic parameters were evaluated.

GRAPHICAL ABSTRACT

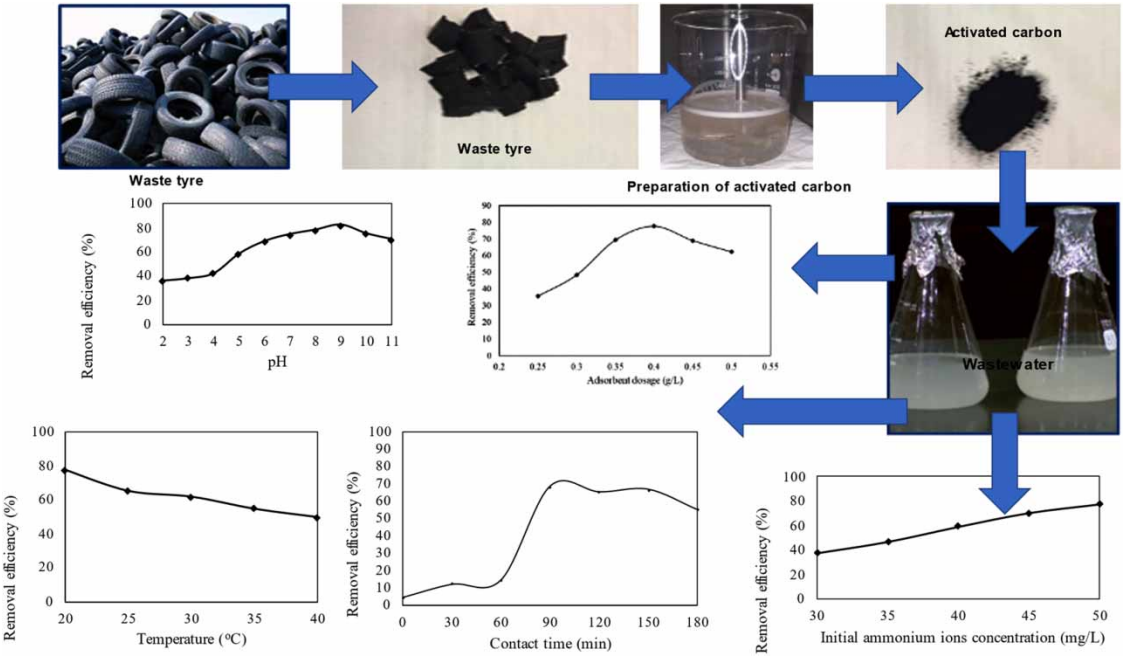

1. INTRODUCTION

Ammonia nitrogen (NH_4^+-N) was found to be the main nitrogen pollutant in wastewater. The presence of pollutants in wastewater affects the life of organisms and may damage all ecosystems (Alardhi *et al.* 2020; Kadhum *et al.* 2021). Excessive ammonia nitrogen concentration is harmful to aquatic life. Therefore, the removal of NH_4^+-N from wastewater is important in the alleviation of environmental problems such as eutrophication and algae blossoms (Chen *et al.* 2021; Kabuba *et al.* 2022). The physical, chemical and biological methods such as air stripping, membrane technology, ion exchange, adsorption, struvite precipitation, electrochemical oxidation, nitrification and denitrification, simultaneous nitrification and denitrification, anaerobic ammonium oxidation and microbial fuel cells have been developed for the removal of ammonia nitrogen from wastewater (Albayati & Doyle 2014; Cho *et al.* 2020; Ren *et al.* 2021; Ali *et al.* 2022). However, these methods have shortcomings such as high operational costs, high sensitivity to process parameters, generation of more wastes that involve additional treatment and disposal, formation of fouling on equipment surfaces and low ammonia removal efficiency (Dong *et al.* 2019). Recently, the adsorption of ammonia nitrogen using activated carbons has been given great attention. Activated carbons have numerous advantages such as a large surface area, a highly developed porous structure, and the possibility to modify the porous structure and surface chemistry to adjust it for a special application (Gonçalves *et al.* 2011). Due to the high cost of commercially produced activated carbons, many researchers have been interested in developing activated carbons using low-cost waste materials with a high carbon content and a low inorganic matter. Different materials such as wood, corn corb, olive stones, lignite, coconut shells, fruit stones, nutshells, rice straw and waste tea have been developed (Yorgun & Yıldız 2015). Recently, Ren *et al.* (2021) modified the activated carbon with iron to improve the adsorption efficiency of ammonia nitrogen in low-temperature wastewater. Therefore, waste tyres represent another interesting source to produce activated carbons since they have high carbon content. Production of activated carbon from waste tyres also solves the problem of environmental pollution (Ariyadejwanich *et al.* 2003). According to a survey of previously published research, there is no work on the removal of ammonia nitrogen from wastewater using activated carbon prepared from waste tyres. The aim of this work is to explore a new adsorbent material for the removal of ammonium nitrogen from wastewater using activated carbon prepared from waste tyres. The effect of process parameters such as adsorbent dosage, contact time, initial ammonium concentration, pH and temperature were studied. The isotherms, kinetic and thermodynamic parameters were evaluated to examine the controlling mechanism of the adsorption process.

2. MATERIALS AND METHODS

2.1. Materials

Waste tyre pyrolysis char (WTPC) was obtained from a local company. WTPC was sieved and only the fraction of particle sizes between 0.5 and 2 mm were selected for the preparation of activated carbons (ACs). NH_4Cl (99.5%) and deionized water were used for the preparation of stock solutions. NaOH (95%) and HCl (35–38%) were used to adjust the pH. All the reagents and chemicals used in the present work were of analytical grade and were acquired by Merck.

2.2. Preparation of activated carbon

The waste tyre char was washed with distilled water to remove impurities and dried for 24 h at 110 °C in the oven. During physical activation, 100 g of waste tyre char sample was loaded into a quartz crucible, and placed in the middle of the quartz tubular reactor. The reactor was inserted inside a tube furnace. The furnace was fitted with a thermometer to measure the inside temperature. The reactor was first purged with nitrogen gas for 1 h to eliminate the presence of oxygen and to generate the inert conditions required for activation. The furnace was then heated from room temperature to 925 °C under an N_2 atmosphere, with a heating rate of 5 °C/min and N_2 flowrate of 200 mL/min. When the temperature inside the reactor was 925 °C, N_2 gas was replaced with steam at the flow rate of 500 mL/min which was supplied by the steam generator. The waste tyre char was activated for 240 min. After activation, the furnace was allowed to cool down to room temperature, and the produced activated carbon was withdrawn from the reactor, ground and sieved to <100 μm. After sieving, the sample was washed with distilled water to remove impurities and dried in the oven at 110 °C for 24 h.

2.3. Adsorbent characterization

The prepared waste tyre char-activated carbon surface area and total pore volume were measured using Brunauer–Emmett–Teller (BET) analysis (Abbood *et al.* 2023; Tanga *et al.* 2023). The total pore volume (V_{Tot}) was obtained from the nitrogen adsorption isotherm at $P/P_o = 0.97$. The t-method was applied to determine the micropore volume (V_{micro}) of the external surface area. The mesopore volume (V_{meso}) was calculated according to Equation (1). The surface properties of the prepared waste tyre char-activated carbon are shown in Table 1.

$$V_{meso} = V_{Total} - V_{micro} \tag{1}$$

Table 1 | The surface properties of the prepared waste tyre char-activated carbon

Sample	S_{BET} (m^2/g)	S_{ext} (m^2/g)	V_{Total} (cm^3/g)	V_{micro} (cm^3/g)	V_{meso} (cm^3/g)	R^2
AC925-240	722	198.5	0.78	0.18	0.44	0.99

2.4. Adsorption studies

Batch experiments were performed in a stirred glass flask of 500 mL to study the ammonium nitrogen adsorption on waste tyre-activated carbon from wastewater solutions. To prepare ammonium nitrogen stock solution, 3.819 g of NH_4Cl was dissolved in 1 L of deionized water with a concentration of 1 mg/mL. The stock solution was continuously diluted with deionized water to achieve the required concentration. The adsorption batch experiments were conducted by taking different masses of waste tyre-activated carbon with 50 mL of synthetic ammonium nitrogen solution at the required solution temperature, initial ammonium concentration, solution pH and contact time. The flasks were covered with stoppers and stirred in a shaking incubator at a constant speed of 200 rpm for different required contact times to ensure equilibrium between ammonium nitrogen and waste tyre-activated carbon. During the experiments, the contact time was varied from 30 to 180 min, pH from 2 to 11, adsorbent dosage from 0.25 to 0.5 g/L, temperature from 20 to 40 °C and initial ammonium concentration from 30 to 50 mg/L. The liquid samples were withdrawn regularly and filtered through a 125-μm sieve. The filtered samples were analyzed by spectrophotometer to determine the changes in ammonium nitrogen concentration in the wastewater solution during the experiments. The removal efficiency of ammonium nitrogen from wastewater onto waste tyre-activated carbon was calculated using Equation (2) (Abdel-Rahman *et al.* 2016; Abu-Dief &

Zikry 2018; Abu-Dief *et al.* 2021a, 2021b):

$$NH_4^+ \text{ removal efficiency } (\%) = \frac{C_e - C_0}{C_e} \times 100 \quad (2)$$

where C_o and C_e are the initial and equilibrium concentration of ammonium nitrogen in wastewater (mg/L), respectively. The pH was adjusted by adding 0.1 M of HCl and NaOH to the wastewater solution.

3. RESULTS AND DISCUSSION

3.1. Characterization of activated carbons

Table 2 presents the operation conditions during the activation tests where the steam flowrate and the heating rate were kept constant, whereas activation temperature and time varied. The activation yields were contracted with expanding temperature for all activation periods. The carbons activated with steam at 900, 925 and 950 °C were labelled by series codes, namely AC900, AC925 and AC950, respectively. The individual samples were then labelled using their series code followed by their activation time (in hours). Activation yield was calculated according to Equation (3).

$$\text{Yield of activated carbon } (\%) = \frac{\text{Weight of activated carbon}}{\text{Weight of WTPC}} \times 100\% \quad (3)$$

Table 2 | Operation conditions during activation tests

Activation					
Run	**Steam flowrate (mL/min)**	**Heating rate (°C/min)**	**Temperature (°C)**	**Time (min)**	**Activation yield (%)**
1	500	5	900	120	73.40
2	500	5	900	240	54.96
3	500	5	925	120	65.32
4	500	5	925	240	49.85
5	500	5	950	120	58.44
6	500	5	950	240	42.68

When the activation time was 120 min, the yield decreased from 73.40 to 65.32% when the temperature increased from 900 to 925 °C, and further decreased to 58.44 when the temperature increased from 925 to 950 °C. The same trend occurred when the activation time was set to 180 and 240 min when the temperature was increased from 900 to 950 °C. This might be due to the dependency of the reaction rate on the activation temperature as the reaction constant k changes with temperature according to the Arrhenius law (Aquilanti *et al.* 2010). Moreover, when the actuation temperature expanded, more compounds will be vaporized, coming about in a diminish within the mass of enacted carbon relative to the initial mass of tyre char. Expanded burn-off in turn reduced the activation yields. At 900 °C, the activation yield was reduced from 73.4 to 54.96% when the activation time was varied from 120 to 240 min. Correspondingly, the yield declined from 65.32 to 49.85% at 925 °C when the activation time was increased from 120 to 240 min. A further decline of activation yield was revealed at 950 °C when the activation time was increased from 120 to 240 min, which declined from 58.44 to 42.68%. This was due to the fact that a longer activation time gave more carbon exposure to react with steam, hence higher reaction took place (Mui *et al.* 2010).

3.1.1. Elemental analysis of tyre char and prepared activated carbons

Carbon content did not show a huge change after activation for all the various temperatures and activation times. The significant change in carbon content was only noticed at the activation temperature and time of 950 °C and 240 min, decreasing from 81.8 to 73.6%. The oxygen (and other) contents are calculated by difference, and it is shown in Figure 1 that their concentrations are increasing when both activation temperature and time increase.

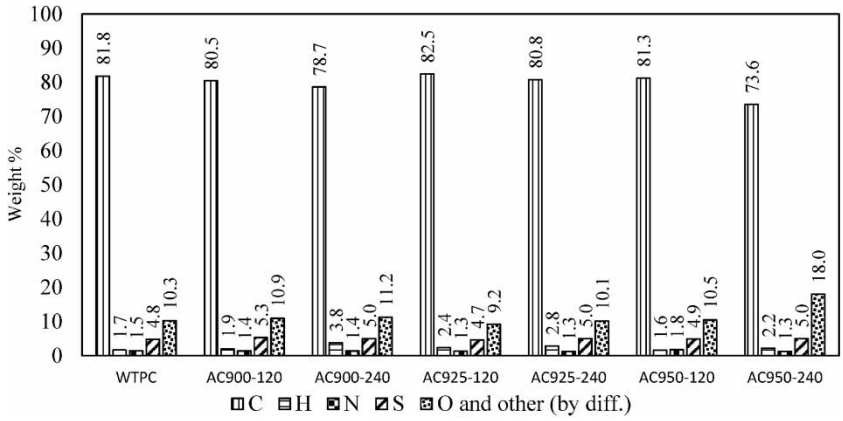

Figure 1 | Elemental analysis of tyre char and prepared activated carbons.

Sulphur content did not show any change for all activation temperatures and activation times. This can be explained by the collapse of tyre char pore structure during high temperatures which changes the solid ash matrix structure and inhibits the release of sulphur. Also, from a theoretical point of view, the carbon–sulphur complex is relatively stable even at high temperatures (i.e., 975 °C), hence, sulphur cannot be easily removed (Bandosz 2006). The sulphur removal results contradict researchers' studies which mentioned that the removal percentage increased with an increase in produced activated carbon yield (Chan *et al.* 2011).

3.1.2. Ash content

Ash content characterizes the incombustible material left after a sample of carbon is completely burned. Figure 2 demonstrates the ash contents of pyrolysis waste tyre char and carbons activated at different temperatures and activation times using steam under a nitrogen atmosphere. The ash contents increased after activation at different temperatures, increasing from 18.6 to 36.8% when the activation temperature was increased from 900 to 950 °C. Increasing activation time also showed an increase in the ash content. Since most of the inorganic matter present in the tyre char was converted to activated carbon during activation and could not be converted into gaseous matter because of their higher boiling temperatures than the activation temperature. The ash contents were also calculated by assuming that there is no loss of ash content from waste tyre char during activation. Figure 2 shows that all calculated ash content values are greater than the measured ash contents, varying from 30.2 to 39.5%. It can be concluded that some components such as metal oxides which have lower boiling points than the activation temperatures evaporated during activation.

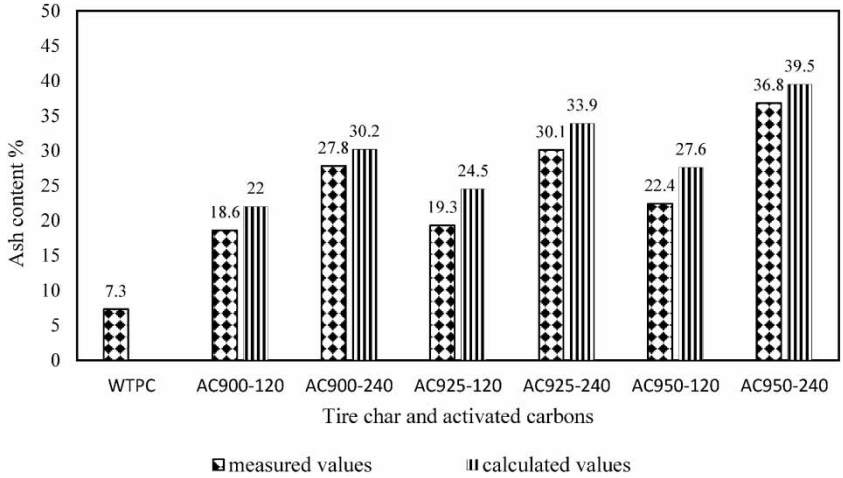

Figure 2 | Ash contents of WTPC and carbons activated at different temperatures and activation times.

3.1.3. Porous properties of WTPC and prepared activated carbons

The textural characterization properties of tyre char and activated carbons were examined by N_2 adsorption at 77 K. Adsorption–desorption isotherms of nitrogen on activated carbons (AC900-120, AC900-240, AC925-120, AC925-240, AC950-120 and AC950-240) samples are shown in Figures 3–5, where q and P/P_o are the amount of N_2 adsorbed and relative pressure, respectively. The activated carbons showed higher adsorption capacities

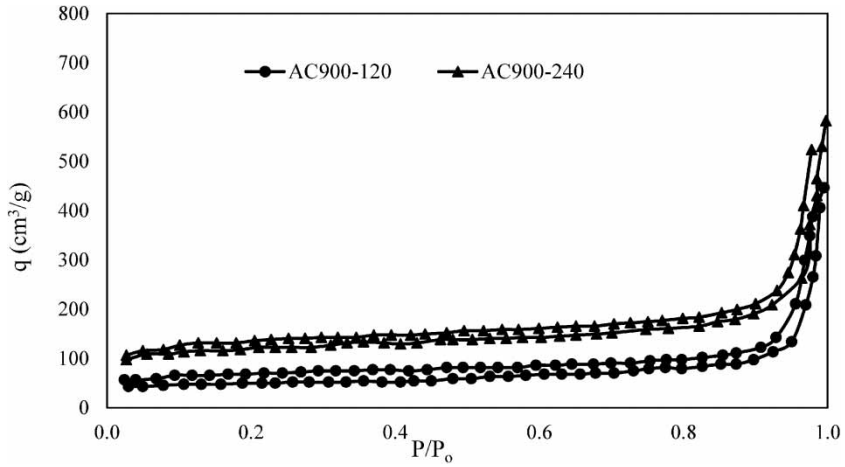

Figure 3 | N_2 adsorption–desorption isotherms (77 K) of activated carbons from steam activation at 900 °C.

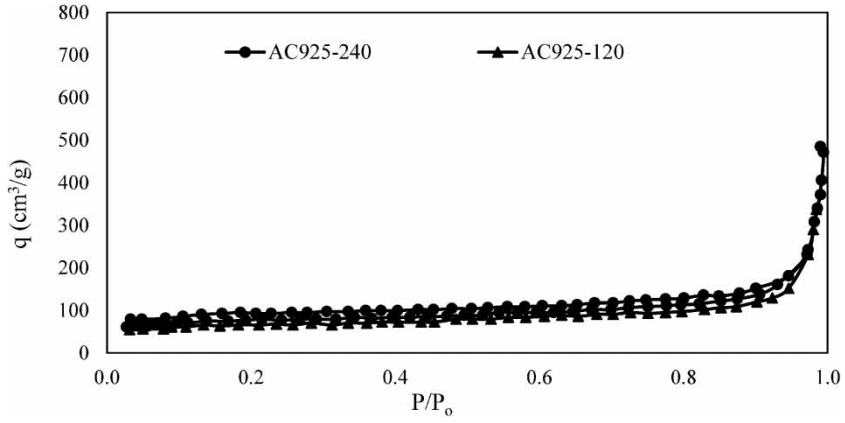

Figure 4 | N_2 adsorption–desorption isotherms (77 K) of activated carbons from steam activation at 925 °C.

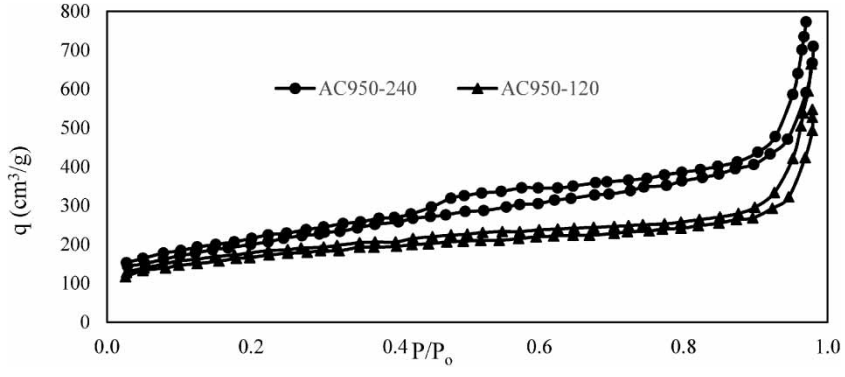

Figure 5 | N_2 adsorption–desorption isotherms (77 K) of activated carbons from steam activation at 950 °C.

at low relative pressure, demonstrating the existence of a more established micropore structure. From Table 3, the activated carbons showed a high mesoporous volume compared to WTPC, which confirms the mesoporous properties of the activated carbons. The International Union of Pure and Applied Chemistry (IUPAC) classification for such isotherms classifies them as Type IV which shows a hysteresis loop at relative pressures of greater than 0.4, indicating a mesoporous carbon. From Figure 4, it is shown that as the activation temperature was increased, the isotherms demonstrate a broadening of the microporosity and higher mesoporosity.

Porous characteristics of WTPC and various prepared activated carbons are shown in Table 3. WTPC had a lower BET surface area and total volume of 32 m^2/g and 0.03 cm^3/g, indicating its non-porous structure. Steam activation of WTPC under a nitrogen atmosphere showed a significant effect on the BET surface area (S_{BET}) and total pore volume (V_{Tot}) as shown in Table 3. Both S_{BET} and V_{Tot} increased with increasing activation time under the same activation temperature. When the activation temperatures were kept constant at 900, 925 and 950 °C while varying the activation time from 120 to 240 min, the BET surface area increased from 238 to 587 m^2/g, 315 to 722 m^2/g and 457 to 725 m^2/g, respectively. Similarly, the total pore volume increased from 0.41 to 0.67 cm^3/g, 0.42 to 0.78 cm^3/g and 0.49 to 0.88 cm^3/g, respectively.

Table 3 | BET surface area and total pore volume (at $P/P_o = 0.97$) of tyre char-activated carbons by the multipoint BET method

WTPC and activated carbons	S_{BET} (m^2/g)	V_{Tot} (cm^3/g)
WTPC	32	0.03
AC900-120	238	0.41
AC900-240	587	0.67
AC925-120	315	0.42
AC925-240	722	0.78
AC950-120	457	0.49
AC950-240	725	0.88

The activation temperature also had a substantial effect on both S_{BET} and V_{Tot}. When the activation times were kept constant at 120 and 240 min while varying the activation temperature from 900, 925 and 950 °C, the BET surface area increased from 238 to 457 m^2/g and 587 to 725 m^2/g, respectively. Correspondingly, the total pore volume increased from 0.41 to 0.49 cm^3/g and 0.67 to 0.88 cm^3/g, respectively.

The t-method was used to determine the external surface areas (S_{ext}) and micropore volumes (V_{mic}), and the results are presented in Table 4. Some modified adsorbent materials such as SBA-15, MCM-41, NH_2/MCM-41 and MCM-48 for aquatic pollutants are compared and presented in Table 5.

Table 4 | External surface areas, micropore volumes and calculated mesopore volumes of tyre char-activated carbons using the t-method

Samples	S_{ext} (m^2/g)	V_{mic} (cm^3/g)	V_{mes} (cm^3/g)	V_{Tot} (cm^3/g)	R^2
WTPC	32	0.0	0.18	0.18	0.97
AC900-120	93.8	0.12	0.38	0.41	1.00
AC900-240	209.6	0.28	0.41	0.67	0.99
AC925-120	105.3	0.17	0.37	0.42	1.00
AC925-240	198.5	0.18	0.44	0.78	0.99
AC950-120	215.6	0.19	0.39	0.49	0.99
AC950-240	529.5	0.14	0.60	0.88	1.00

3.1.4. Scanning electron microscope

The morphological structures of waste tyre char and all prepared waste tyre-activated carbons were characterized using scanning electron microscope (SEM). Figures 6–12 show the SEM of WTPC AC900-120, AC900-240, AC925-120, AC925-240, AC950-120 and AC950-240, respectively. From Figure 6, WTPC showed the absence of microporosity, and it is inconsistent with those previously reported (López *et al.* 2013). The development of

Table 5 | Comparative structure properties with some adsorbent materials

WTPC and activated carbons	S_{BET} (m^2/g)	V_{Tot} (cm^3/g)	References
WTPC	32	0.03	This study
AC950-240	725	0.88	This study
SBA-15	845.42	0.854	Atiyah *et al.* (2022a)
MCM-41	1,200	0.7395	Atiyah *et al.* (2022b)
NH_2/MCM-41	11.954	0.00867	Atiyah *et al.* (2022b)
MCM-48	1,120	0.678	Sastre *et al.* (2016)

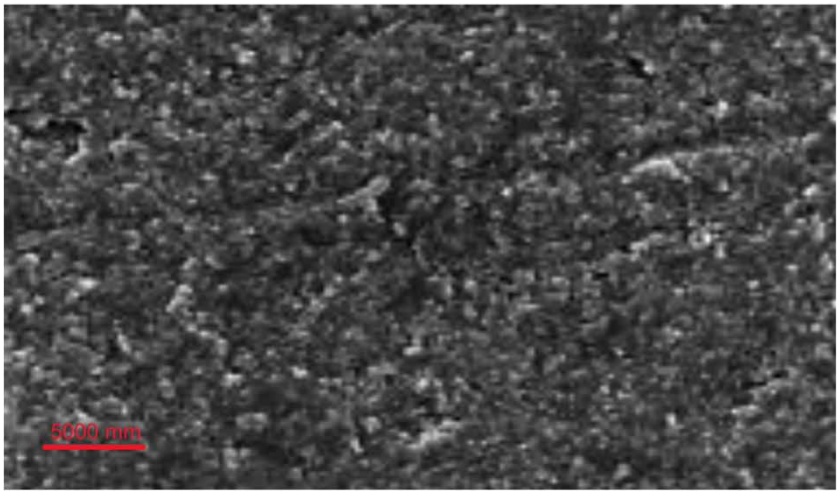

Figure 6 | SEM image for WTPC, magnification 5,000.

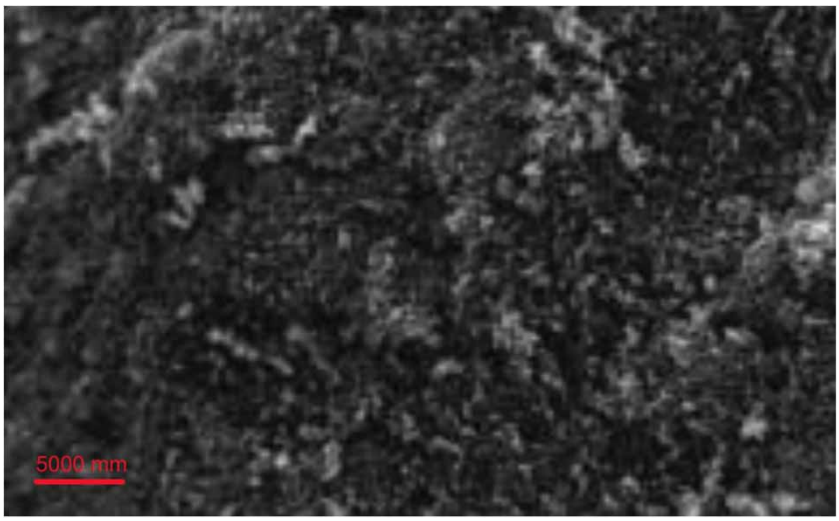

Figure 7 | SEM image for AC900-120, magnification 5,000 ×.

micropores and mesopores was observed when the temperature and activation time increased. The same observation was reported previously by different researchers (Fernandez *et al.* 2012). However, a gradual change in the size of the clusters in each micrograph was noticed. WTPC has the biggest cluster, followed by AC900-125. The

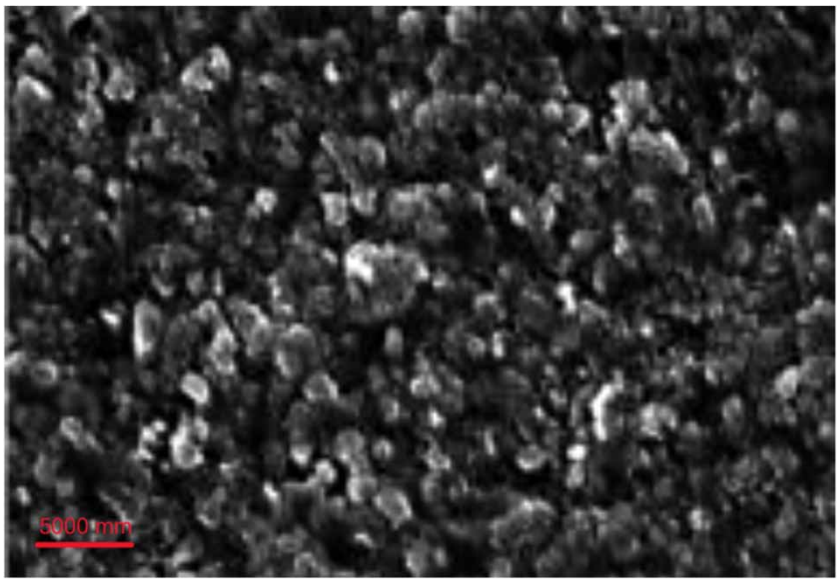

Figure 8 | SEM image of AC900-240, magnification 5,000 ×.

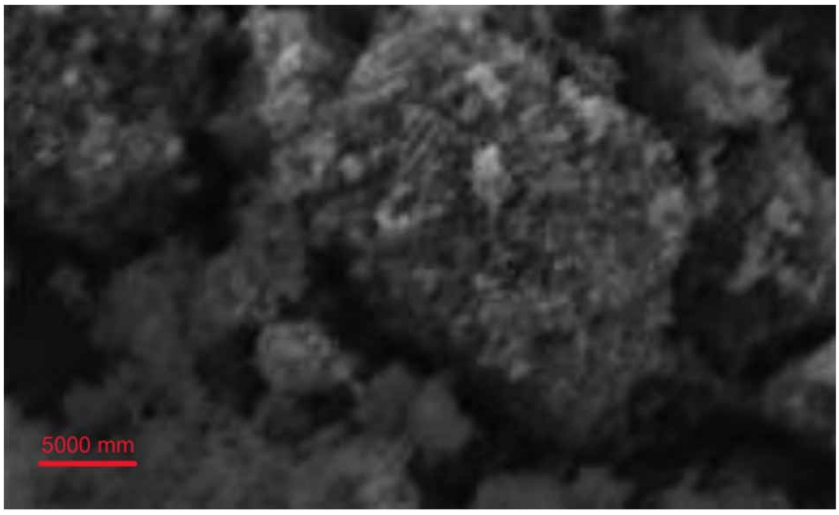

Figure 9 | SEM image of AC925-120, magnification 5,000 ×.

AC950-120 and AC950-240 have the smallest cluster. Suuberg & Aarna (2007) reported that for a unit area, the more the number of clusters and smaller the size of a cluster, the higher the BET surface should be, which agrees with the BET results in this study.

3.2. The effect of adsorbent dosage

The effect of the tyre char-activated carbon dosage on ammonia nitrogen adsorption at 25 °C is shown in Figure 13. The dosage of the adsorbent was varied between 0.25 and 0.5 g/L in a 50-mL wastewater solution with an initial concentration of ammonium at 50 mg/L at 25 °C for 60 min. It is shown from Figure 13 that the rate of ammonia nitrogen removal increased with an increase in adsorbent dosage. This was due to the fact that the more adsorbent was added, the greater the total specific surface area provided for the adsorption of ammonia nitrogen was, thus increasing the removal rate (Bhandari & Gogate 2018). The percentage removal of ammonium nitrogen increased from 35 to 77% when the adsorbent dosage was increased from 0.25 to 0.4 g/L. Nevertheless, more increase in adsorbent dosage from 0.40 to 0.5 g/L resulted in a decrease in ammonium nitrogen removal from 77 to 52% due to the accumulation of particles and shielding of active sites at higher dosages.

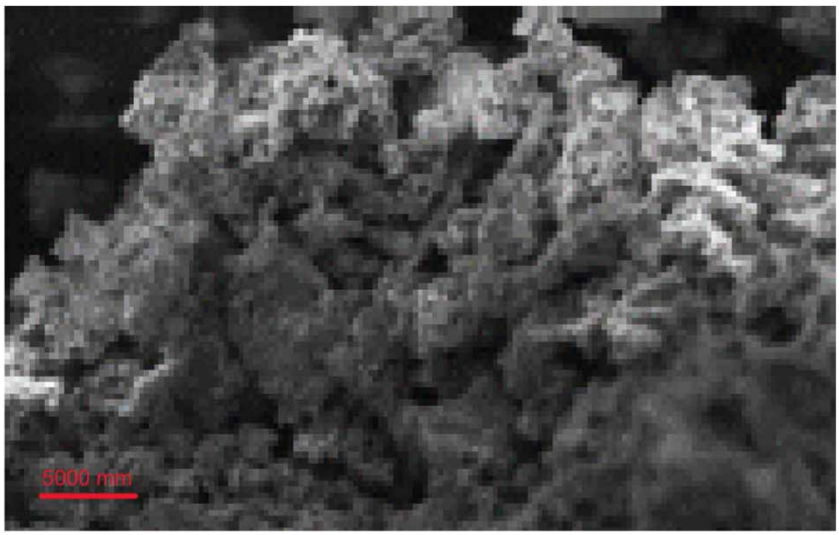

Figure 10 | SEM image of AC925-240, magnification 5,000 ×.

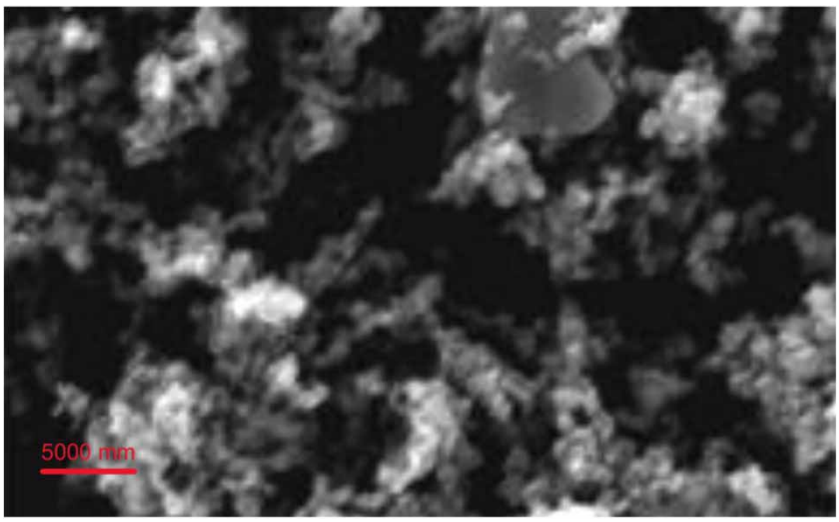

Figure 11 | SEM image of AC950-120, magnification 5,000 ×.

Figure 12 | SEM image of AC950-240, magnification 5,000 ×.

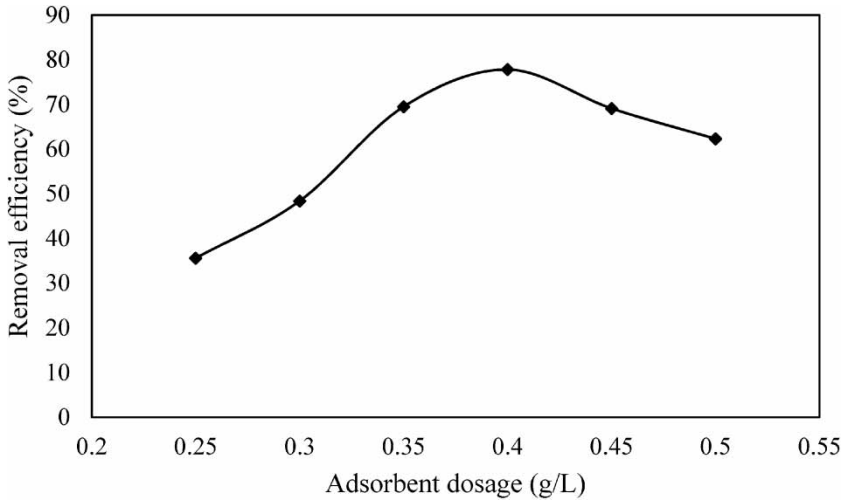

Figure 13 | The effect of the tyre char-activated carbon dosage on ammonia nitrogen adsorption.

Also, as the ammonia nitrogen concentration in the wastewater solution was reduced, and the adsorption driving force was also reduced (Ren *et al.* 2021).

3.3. The effect of pH

The removal of ammonium nitrogen from wastewater by adsorption is highly dependent on the pH of the solution since it can affect the extent of NH_4^+ ionization as well as the surface characteristics of an adsorbent. The effect of pH on the adsorption of ammonium nitrogen by waste tyre-derived activated carbon was investigated and the results are shown in Figure 14. It was observed that the percentage removal of ammonium nitrogen increased when pH was increased from 5 to 9, with the maximum removal percentage of 82.3% at pH 9. The percentage removal of ammonium nitrogen decreased when pH was decreased from 5 to 2, with the minimum removal percentage of 36.5% at pH 2. This was due to the excess H^+ ions in the solution which competed with the NH_4^+ ions for the active adsorption sites. The percentage removal started to decrease from 82.3 to 70.5% when the pH was further increased from 9 to 11. At pH greater than 9, the removal of NH_4^+ decreases because the reaction favours the formation of NH_3, which cannot be exchanged onto the adsorbent. A similar trend for the adsorption of ammonium nitrogen onto different adsorbents was observed by different researchers (Yian *et al.* 2012).

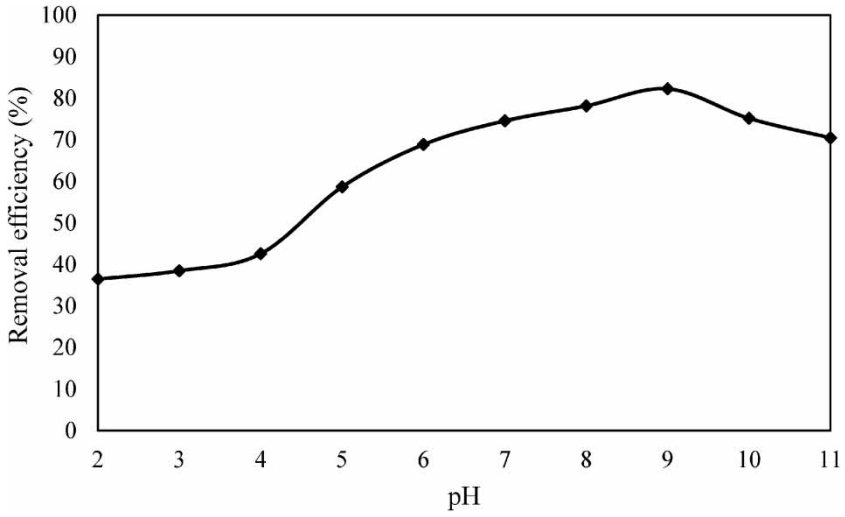

Figure 14 | The effect of pH on ammonia nitrogen adsorption.

3.4. The effect of temperature

The effect of temperature on ammonium nitrogen adsorption on waste tyre-activated carbon was investigated and the results are shown in Figure 15. All parameters were kept constant, i.e., pH at 9, adsorbent dosage at 0.4 g/L, initial ammonium nitrogen at 50 mg/L and contact time of 60 min. Temperature was varied between 20 and 40 °C. From Figure 15, the percentage removal of ammonium nitrogen decreased with an increase in temperature from 20 to 40 °C. The maximum removal of ammonium nitrogen was achieved at 20 °C, which was 78%. The minimum removal of ammonium nitrogen was 50.4% at 40 °C. A similar trend was shown by the work conducted by Sabah *et al.* (2002), which reported that ammonium nitrogen exchange capacity was more favourable at lower temperatures. Theoretically, the rate of adsorption is directly proportional to the process temperature. However, too high a temperature is in favour of an exothermic reaction once it reaches the equilibrium. Thus, ammonium nitrogen tends to desorb from the adsorbent to the solution phase when the temperature is too high (Karadag *et al.* 2006). Furthermore, an increase in temperature increases the rate of solute movement in the bulk solution and decreases the retarding forces acting on the adsorbate ions (Boopathy *et al.* 2012).

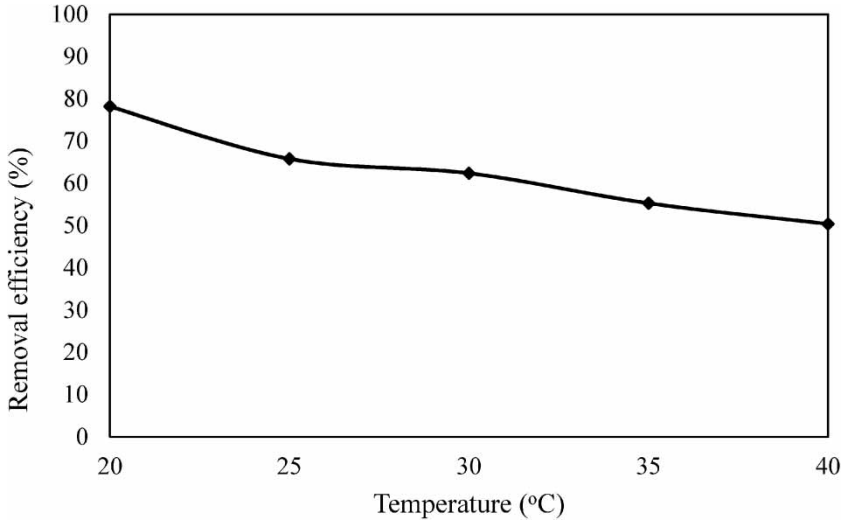

Figure 15 | The effect of temperature on ammonia nitrogen adsorption.

3.5. The effect of contact time

Contact time is another factor that affects the adsorption of ammonium nitrogen onto waste tyre char-activated carbon. It can have a significant effect on the economic effectiveness of the process and adsorption kinetics (Srivastava *et al.* 2016). Figure 16 presents the effect of contact time on ammonium nitrogen adsorption onto

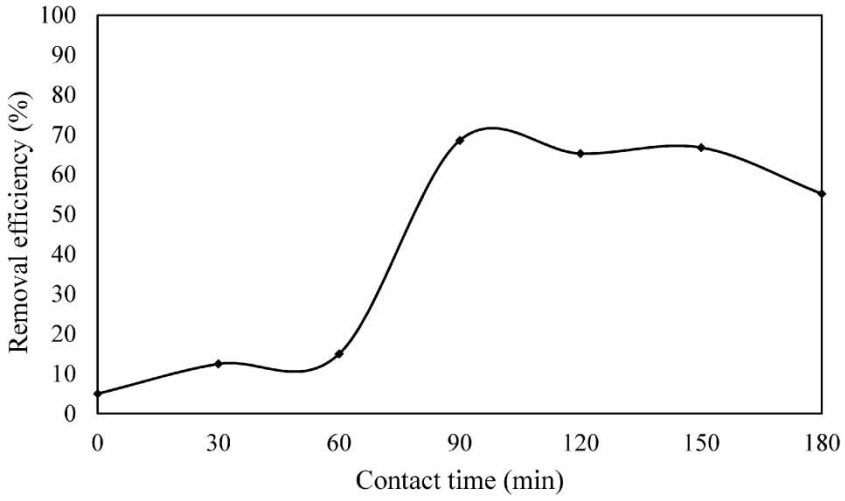

Figure 16 | The effect of contact time on ammonia nitrogen adsorption.

waste tyre-activated carbon with an initial ammonium concentration of 50 mg/L in wastewater solution, pH of 9, an adsorbent dosage of 0.4 g/L and solution temperature of 25 °C. Ammonium nitrogen adsorption started to be slow between 0 and 60 min. The adsorption process accelerated between 60 and 90 min, with the highest percentage of removal achieved at 90 min which was 68.6%. That was since the high number of unoccupied adsorption sites were still available, and the solute concentration gradient of the adsorption process was high, encouraging the fast initial uptake (Yang *et al.* 2018). The process was at equilibrium between 90 and 150 min with removal percentage of ammonium nitrogen ranging between 68.6 and 66.8%, and removal percentage of ammonium nitrogen started to decline from 66.8 to 55.2% between 150 and 180 min. This took place because there was an ionic balance between the wastewater solution and the waste tyre-activated carbon adsorbent. Also, the remaining vacant adsorption sites were not easy to be filled due to the repulsive force from NH_4^+.

3.6. Effect of initial ammonium concentration

The effect of initial concentration on the adsorption of ammonium nitrogen onto waste tyre char-activated carbon was examined and the results are shown in Figure 17. The initial ammonium concentration in the wastewater solution was varied from 30 to 50 mg/L. The other parameters were kept constant, pH at 7, adsorbent dosage at 0.4 g/L, temperature at 20 °C and contact time at 90 min. The results show that the removal percentage of ammonium nitrogen increases from 38 to 77% with an increase in initial ammonium concentration from 30 to 50 mg/L in wastewater solution. This can be explained by the mass transfer stimulus between the wastewater solution and the surface of waste tyre char-activated carbon. Also, the ammonium nitrogen concentration on the surface of activated carbon in equilibrium with the ammonia in the wastewater solution increases with its concentration in the solution. By increasing the initial ammonium concentration, the mass transfer driving force and the rate at which ammonium ions pass to the surface of the waste tyre char-activated carbon also increased. Consequently, the ammonium nitrogen could transfer from the external surface to the internal micropores of the waste tyre char-activated carbon (Kotoulas *et al.* 2019). When the initial concentration of ammonium ions is low, ammonium ions could first exchange with cations on the external surface of the waste tyre char-activated carbon and only after that it would exchange in the internal surface of the waste tyre char-activated carbon (Vaičiukynienė *et al.* 2020).

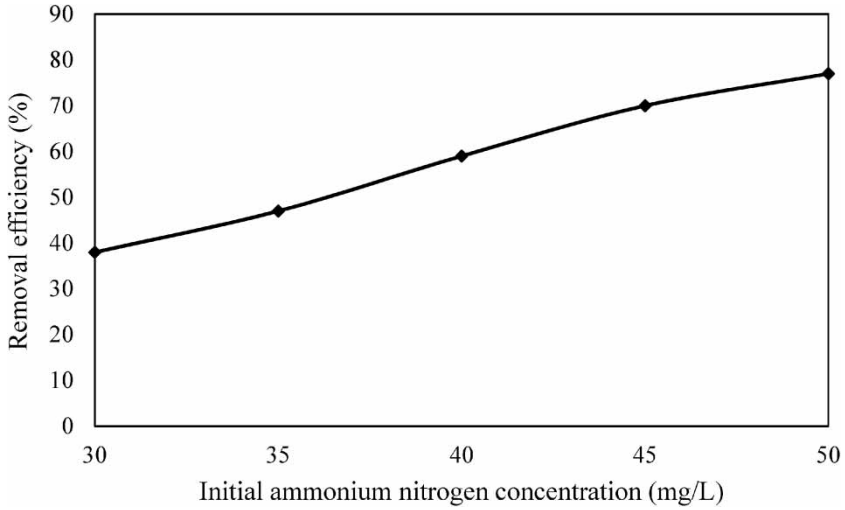

Figure 17 | The effect of initial concentration on ammonia nitrogen adsorption.

3.7. Adsorption kinetics

Kinetics analysis is an important method for identifying the limiting-velocity procedure in the reaction process. The kinetic models such as pseudo-first-order, pseudo-second-order and intra-particle diffusion were used to investigate the mechanisms of the adsorption process. The adsorption was performed by fitting the experimental data into all three conventional kinetic equations to determine the adsorption rate constant. The first-order kinetic analysis of adsorption is characterized by Lagergren's pseudo-first-order differential Equation (4)

(Ruiz-Baltazar 2018).

$$log(q_e - q_t) = logq_e - t\left(\frac{k_1}{2.303}\right) \tag{4}$$

where q_e and q_t are the amounts of ammonium nitrate adsorbed (mg/g) at equilibrium and time t, respectively. k_1 (l/min) is the rate constant of first-order adsorption. The pseudo-second-order model can be expressed in the form of Equation (5) (Mohamed & Abu-Dief 2018; Abdel-Rahman *et al.* 2019; Abu-Dief *et al.* 2021a, 2021b).

$$\frac{t}{q_t} = \frac{1}{k_2 q_e^2} + \frac{t}{q_e} \tag{5}$$

where k_2 is the pseudo-second-order rate constant (g/mg min), q_e and q_t are the amounts of nitrate adsorbed (mg/g) at equilibrium and time t, respectively.

The fit of these models was checked by each linear plot and results are presented in Figures 18–20. The slope and intercept of the plot of t/q_t vs. t were used to determine pseudo-first-order rate constant k_1 and q_e. Similarly, the slope and intercept of the plot of log $(q_e–q_t)$ vs. t were used to determine pseudo-second-order rate constant k_2 and q_e, and the results are presented in Table 6 together with correlation coefficients (R^2) values. From the results in Table 6, the calculated q_e value is in line with the experimental q_e value for pseudo-first-order kinetic model, with a high correlation coefficient of 0.9783. This urges that the adsorption kinetic could well be estimated more satisfactorily by first-order kinetic model for ammonia nitrogen. The results agree well with other studies which obtained similar outcomes (Cadaval *et al.* 2015; Ren *et al.* 2021).

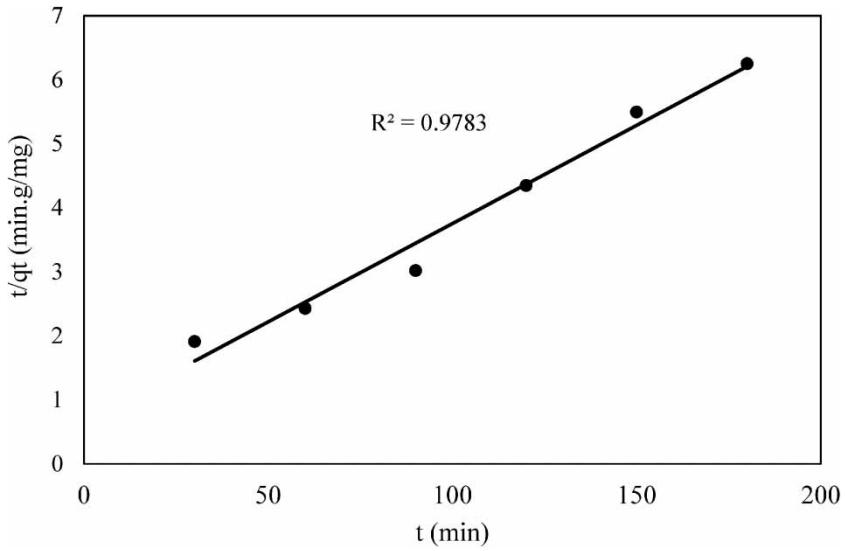

Figure 18 | Pseudo-first-order linear kinetic plot for ammonia nitrogen adsorption.

The intra-particle diffusion rate equation is expressed by the Equation (6).

$$q_t = k_p^{\frac{1}{2}} \tag{6}$$

where k_p is the intra-particle rate constant (g/mg.min$^{1/2}$).

The intra-particle diffusion model showed that the adsorption process of ammonia nitrogen was composed of three stages: ammonia nitrogen first spreads rapidly to the activated carbon surface then diffused into the internal pores, and finally entered the interior of the activated carbon and reduced the pore size. The fitted straight line in Figure 20 deviated from the origin confirming that the adsorption mechanism of ammonia nitrogen onto activated carbon was complicated. The results are presented in Table 7 together with correlation coefficient (R^2) value.

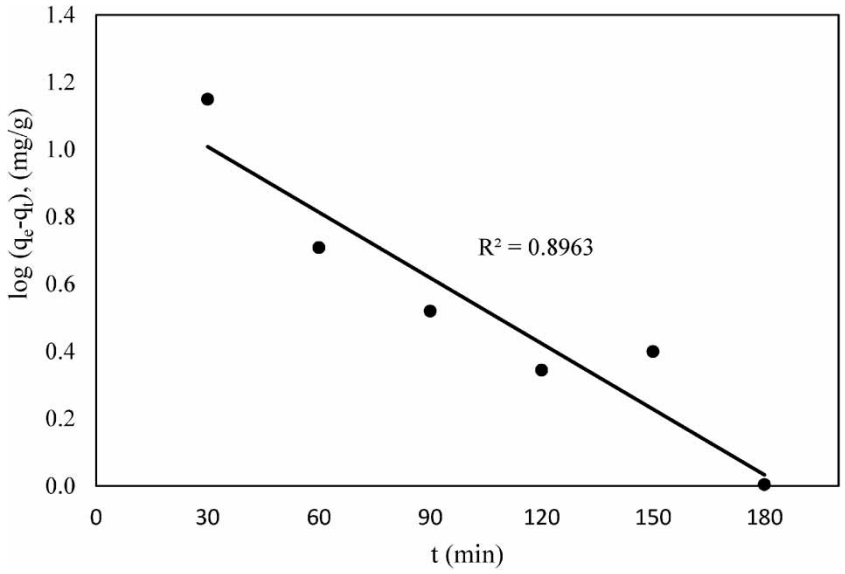

Figure 19 | Pseudo-second-order linear kinetic plot for ammonia nitrogen adsorption.

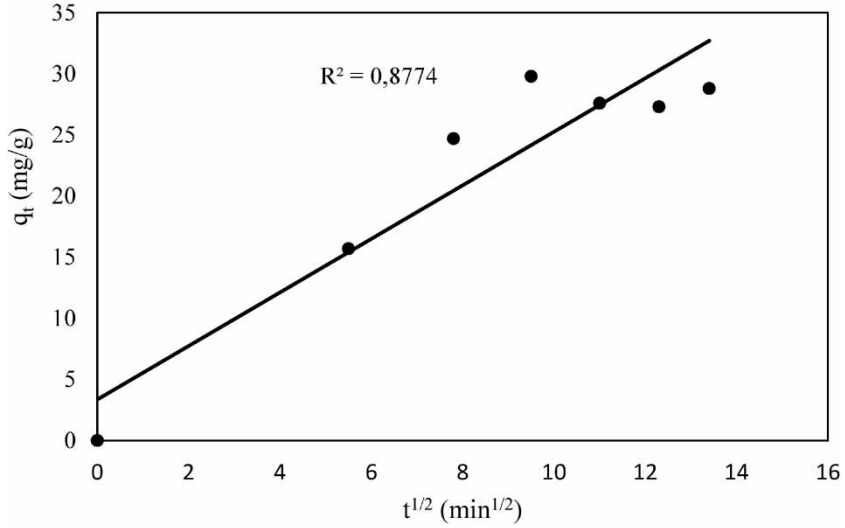

Figure 20 | Intra-particle model linear kinetic plot for ammonia nitrogen adsorption.

Table 6 | Pseudo-first-order and pseudo-second-order kinetic parameters for adsorption rate expressions

	First-order kinetic model			Second-order kinetic model		
$q_{e\ (exp)}$ (mg/g)	k_1 (1/min)	$q_{e\ (calc)}$ (mg/g)	R^2	k_2 (g/mg. min)	$q_{e\ (calc)}$ (mg/g)	R^2
29.8	0.0015	32.57	0.9783	0.00022	3.33	0.8963

3.8. Adsorption isotherms

Adsorption properties and equilibrium are significant to improve the application of adsorbents due to the fact that define how adsorbates interact with adsorbents. The adsorption isotherms represent the adsorption equilibrium data which relate to the relationship between the mass of the solute adsorbed per unit mass of adsorbent, q_e, and the solute concentration in the solution at equilibrium, C_e (Boopathy *et al.* 2012). The experimental data for ammonia nitrogen adsorption onto waste tyre-activated carbon was fitted to determine the equilibrium data of

Table 7 | Kinetic parameters for intra-particle adsorption rate expressions

Intra-particle model	
k_p (g/mg.min$^{1/2}$)	R^2
2.1914	0.8774

adsorption isotherms and the equilibrium curves are shown in Figures 21–26. Adsorption isotherm study was carried out on two isotherm models such as Langmuir and Freundlich. Table 4 presents the obtained isotherm parameters of nitrate adsorption. The Langmuir adsorption isotherm assumes that adsorption takes place at specific homogeneous sites within the adsorbent and has effective application for the monolayer adsorption process, and this can be described by Equation (7).

$$\frac{C_e}{q_e} = \frac{1}{K_L q_m} + \frac{C_e}{q_m} \tag{7}$$

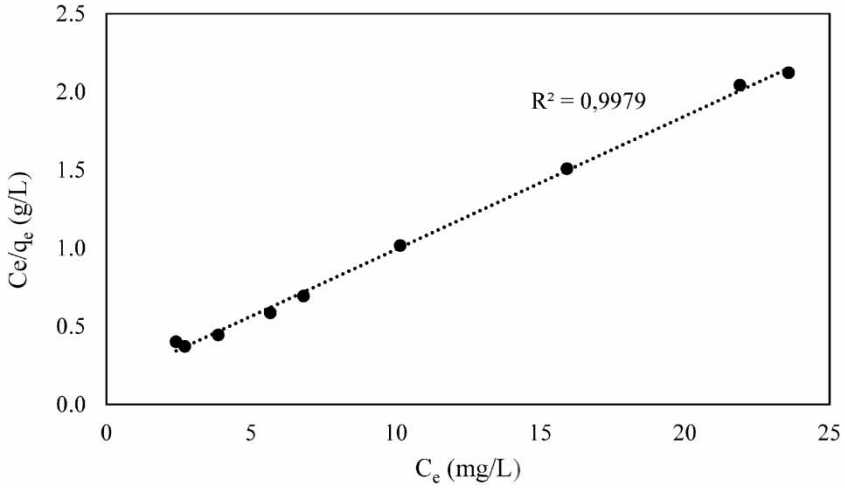

Figure 21 | Langmuir linear adsorption isotherm for adsorption of ammonia nitrogen at 20 °C.

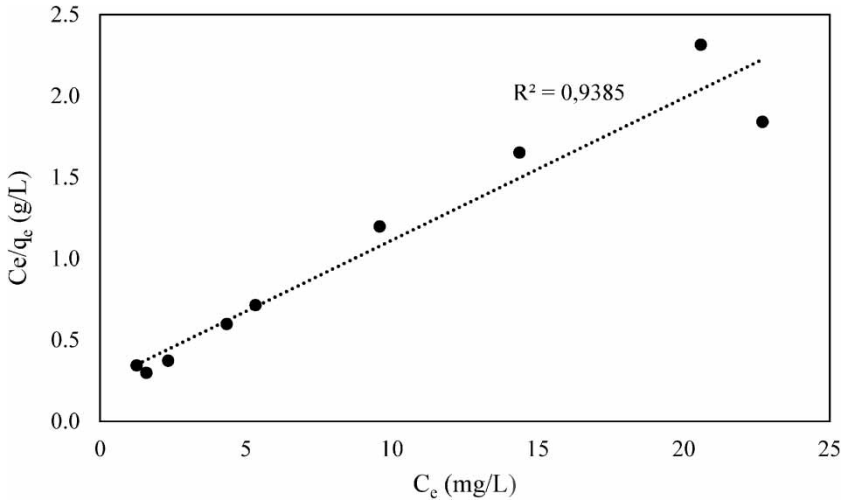

Figure 22 | Langmuir linear adsorption isotherm for adsorption of ammonia nitrogen at 30 °C.

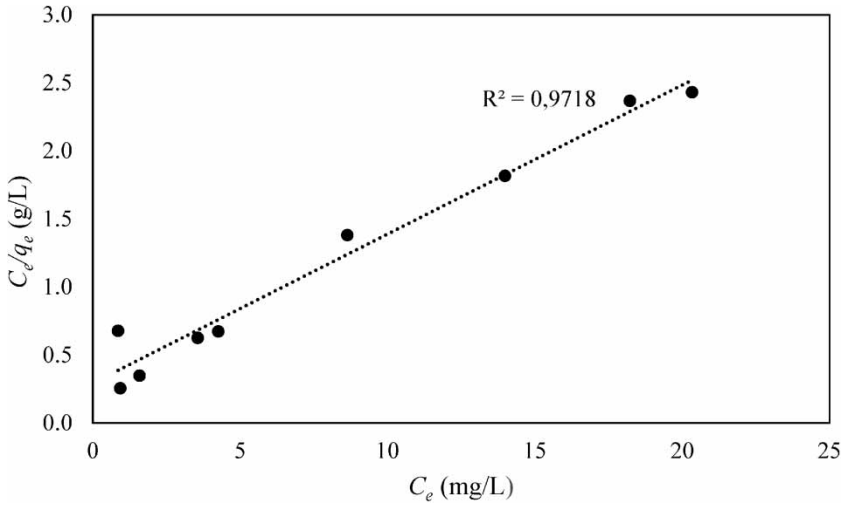

Figure 23 | Langmuir linear adsorption isotherm for adsorption of ammonia nitrogen at 40 °C.

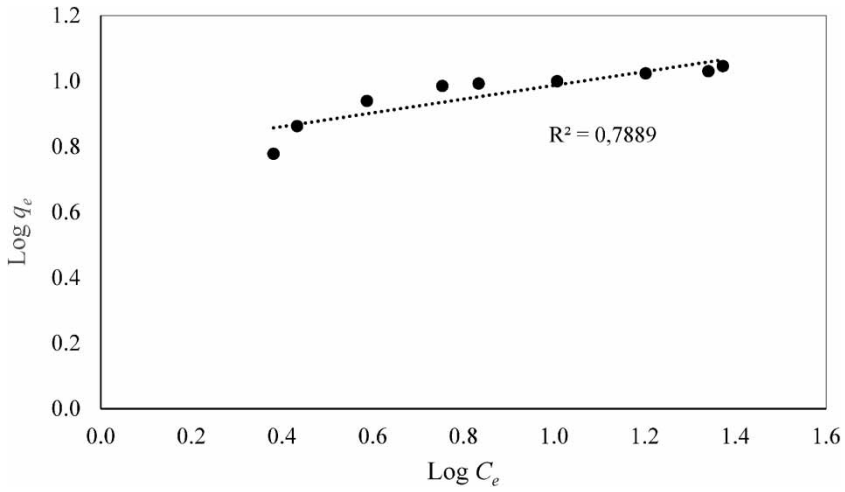

Figure 24 | Freundlich linear adsorption isotherm for adsorption of ammonia nitrogen at 20 °C.

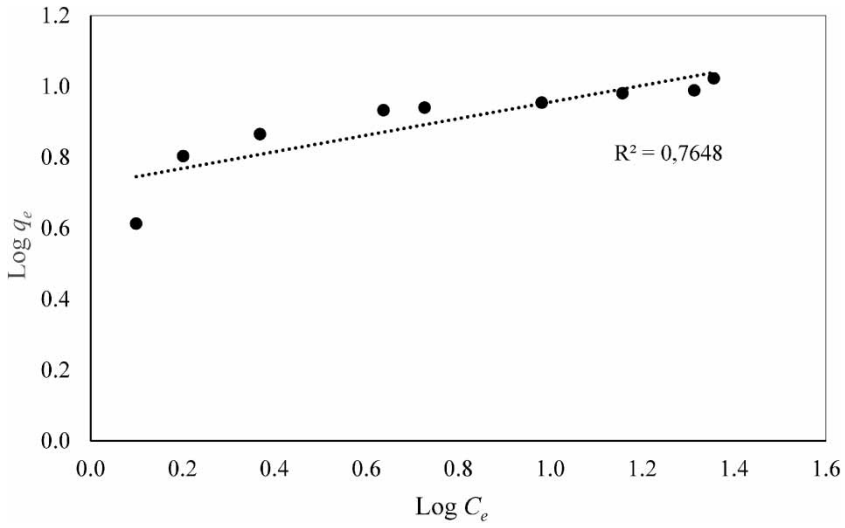

Figure 25 | Freundlich linear adsorption isotherm for adsorption of ammonia nitrogen at 30 °C.

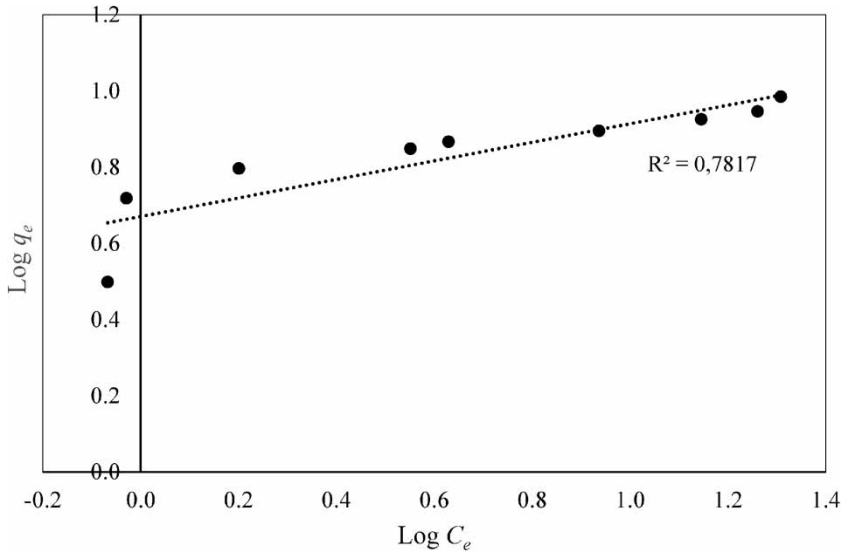

Figure 26 | Freundlich linear adsorption isotherm for adsorption of ammonia nitrogen at 40 °C.

where C_e (mg/L) is the concentration of the molecules at equilibrium, q_e (mg/g) is the amount of nitrate adsorbed on activated carbon, q_m is the maximum adsorption capacity (mg/g) and K_L is the Langmuir constant (L/mg). The plots of C_e/q_e vs. C_e (Figures 9–11) give the adsorption coefficients. On the other hand, the Freundlich equation is an empirical equation based on adsorption on a heterogeneous surface and is not restricted to the formation of the monolayer. Freundlich equation is expressed by Equation (8) (Hameed & Daud 2008; Kabuba & Banza 2021).

$$logq_e = logK_f + \frac{1}{n} logC_e \tag{8}$$

where K_f is adsorption capacity and n is adsorption intensity, and both are Freundlich constants. The slope and intercept from the plots of log q_e vs. log C_e give the Freundlich constants. The results showed that the Langmuir model provided higher linear correlation coefficients compared to the Freundlich model, with correlation coefficients of 0.998, 0.936 and 0.9718 at 20, 30 and 40 °C, respectively. This indicates that the experimental data of the adsorption process is in good agreement with that obtained by the Langmuir isotherm model. This model suggests that ammonia nitrogen adsorption onto waste tyre-activated carbon follows a homogeneous monolayer mechanism. It has also been reported in the literature that the Langmuir isotherm was the best model for the experimental data of ammonia nitrogen adsorption on different adsorbents (Ahmadi *et al.* 2016). Moreover, the value of n greater than 1 shows favourable nature of adsorption (Demiral & Gündüzoğlu 2010). The values of n presented in Table 8 are all greater than 1, indicating that ammonia nitrogen is favourably adsorbed by activated carbon prepared from waste tyres.

Table 8 | Isotherm parameters for the removal of ammonia nitrogen

				Constants		
Isotherms	**Temperature**	**Slope**	**Intercept**	**q_m (mg/g)**	**K_L (L/mg)**	**R^2**
Langmuir	20	0.085	0.138	11.710	7.231	0.997
	30	0.087	0.239	11.442	4.177	0.939
	40	0.110	0.294	9.132	3.401	0.972
		Slope	**Intercept**	**n (mg/g)**	**K_F (L/mg)**	**R^2**
	20	0.210	0.778	4.773	5.995	0.789
	30	0.234	0.772	4.272	5.920	0.765
Freundlich	40	0.244	0.671	4.105	4.684	0.782

3.9. Thermodynamic studies

The thermodynamic parameters such as Gibbs free energy change ($\Delta G°$), enthalpy change ($\Delta H°$) and entropy change ($\Delta S°$) were determined to evaluate the feasibility and nature of the adsorption reaction. The slope and intercept from the plot of ln K_L vs. $1/T$ were used to calculate $\Delta H°$ and ($\Delta S°$). according to Equation (9). Gibbs free energy change ($\Delta G°$) was calculated according to Equation (10).

$$\mathrm{LnK_c} = (\Delta \mathrm{S^o})/\mathrm{R} - (\Delta \mathrm{H^o})/\mathrm{RT} \tag{9}$$

$$\Delta G^{\circ} = -RTlnK_f \tag{10}$$

where R is the universal gas constant (8.314 J/mol.K) and T is the temperature (K). From Table 9, the values of $\Delta G°$ at 20, 30 and 40 °C were found to be −4,819.22, −3,601.41 and −3,185.65, respectively. The negative values of $\Delta G°$ indicate that the adsorption of ammonium nitrogen was spontaneous in nature. Moreover, the occurrence of physical adsorption during the adsorption process is indicated by the values of $\Delta G°$ which are lower than −10,000 J/mol (Hafshejani *et al.* 2016). The negative value of $\Delta H°$ (−28,884.5 J/mol) suggests that the adsorption is exothermic. The results are inconsistent with the previous studies (Mazarji *et al.* 2017). The negative value of $\Delta S°$ (−82.561 kJ/mol K) indicates that there is a decrease in the randomness in the adsorbent/wastewater interface during the adsorption process (Bhatnagar *et al.* 2008).

Table 9 | Thermodynamic parameters

T (K)	$1/T$ (1/K)	K_L	ln K_L	ΔG° (J/mol)	ΔH° (J/K.mol)	ΔS° (J/K)
293	0.00341	7.23	1.98	−4,819,22	−28,884,50	−82.56
303	0.00330	4.18	1.43	−3,601,41		
313	0.00319	3.40	1.22	−3,185,65		

3.10. Comparative study

A comparative study between this research work and the literature can be done by assessing the waste tyre-activated carbon for the removal of ammonium nitrogen using modified adsorbent materials, as shown in Table 5. Table 5 illustrates their structural properties.

4. CONCLUSION

In this study, the adsorption of ammonium nitrogen using waste tyre-activated carbon from the wastewater solution has been studied in batch experiments. The results showed that the optimal conditions for the efficient adsorption of ammonia nitrogen onto waste tyre-activated carbon were found as follows: an adsorbent dosage of 0.4 g/L, pH of 9, temperature of 20 °C, contact time of 90 min and initial ammonium nitrogen concentration of 50 mg/L. The adsorption kinetics are best described by a pseudo-second-order model. The Langmuir isotherm was found to provide the best fit for the experimental data. The negative values of $\Delta H°$ indicate that the adsorption of ammonia nitrogen onto waste tyre-activated carbon was exothermic, negative values of $\Delta G°$ showed the spontaneous nature of the process and positive values of $\Delta S°$ reflect an increase in randomness.

ACKNOWLEDGEMENTS

We are sincerely grateful to the reviewers and the editor for their useful comments that have helped us to improve the quality of our study.

DATA AVAILABILITY STATEMENT

All relevant data are included in the paper or its Supplementary Information.

CONFLICT OF INTEREST

The authors declare there is no conflict.

REFERENCES

Abbood, N. S., Ali, N. S., Khader, E. H., Majdi, H. S., Albayati, T. M. & Saady, N. M. C. 2023 Photocatalytic degradation of cefotaxime pharmaceutical compounds onto a modifed nanocatalyst. *Research on Chemical Intermediates* **49**, 43–56. https://doi.org/10.1007/s11164-022-04879-3.

Abdel-Rahman, L. H., Abu-Dief, A. M., Abd-El Sayed, M. A. & Zikry, M. M. 2016 Nano sized Moringa oleifera an effective strategy for Pb(II) ions removal from aqueous solution. *Chemistry and Materials Research* **6**, 4.

Abdel-Rahman, L. H., Abu-Dief, A. M., Al-Farhan, B. S., Yousef, D. & El-Sayed, M. A. 2019 Kinetic study of humic acid adsorption onto smectite: the role of individual and blend background electrolyte. *AIMS Materials Science* **6**(6), 1176–1190.

Abu-Dief, A. M. & Zikry, M. M. 2018 Adsorption of the heavy metal ions onto bio sorbents: a review. *International Journal of Nanomaterials and Chemistry* **4**(3), 27–39.

Abu-Dief, A. M., Essawy, A. A., Diab, A. K. & Mohamed, W. S. 2021a Facile synthesis and characterization of novel Gd_2O_3–CdO binary mixed oxide nanocomposites of highly photocatalytic activity for wastewater remediation under solar illumination. *Journal of Physics and Chemistry of Solids* **148**, 109666.

Abu-Dief, A. M., Abdel-Rahman, L. H., Abd-ElSayed, M. A. & Zikry, M. M. 2021b Green synthesis of silver nanoparticles using delonix regia extract, characterization and its application as adsorbent for removal of Cu (II) ions from aqueous solution. *Asian Journal of Applied Chemistry Research* **9**(1), 1–15.

Ahmadi, M., Mahvi, A., Doroud, Z., Ramavandi, B. & Teymouri, P. 2016 Kinetic and equilibrium studies of nitrate adsorption from aqueous solution by lewatite *FO* 36. *Journal of Environmental Engineering and Management* **15**, 733–740.

Alardhi, S. M., Alrubaye, J. M. & Albayati, T. M. 2020 *IOP Conference Series: Materials Science and Engineering* **928**, 052020. doi:10.1088/1757-899X/928/5/052020.

Albayati, T. M. & Doyle, A. M. 2014 Purification of aniline and nitro-substituted aniline contaminants from aqueous solution using beta zeolite. *Chemistry: Bulgarian Journal* **23**(1), 105–114.

Ali, N. S., Kalash, K. R., Ahmed, A. N. & Albayati, T. M. 2022 Performance of a solar photocatalysis reactor as pretreatment for wastewater via UV, UV/TiO_2, and UV/H_2O_2 to control membrane fouling. *Scientifc Reports* **12**, 16782. https://doi.org/10.1038/s41598-022-20984-0.

Aquilanti, V., Mundim, K., Elango, M., Kleijn, S. & Kasai, T. 2010 Temperature dependence of chemical and biophysical rate processes: phenomenological approach to deviations from Arrhenius law. *Journal of Chemical Physics Letters* **498**, 209–213.

Ariyadejwanich, P., Tanthapanichakoon, W., Nakagawa, K., Mukai, S. & Tamon, H. 2003 Preparation and characterization of mesoporous activated carbon from waste tires. *Journal of Carbon* **4**, 157–164.

Atiyah, A. N., Albayati, T. M. & Atiya, M. A. 2022a Interaction behavior of curcumin encapsulated onto functionalized SBA-15 as an efficient carrier and release in drug delivery. *Journal of Molecular Structure* **1260**, 132879.

Atiyah, A. N., Albayati, T. M. & Atiya, M. A. 2022b Functionalization of mesoporous MCM-41 for the delivery of curcumin as an anti-inflammatory therapy. *Advanced Powder Technology* **33**, 103417.

Bandosz, T. 2006 *Activated Carbon Surfaces in Environmental Remediation. Interface Science and Technology*. Vol. 7. Academic Press, New York, pp. 1–215.

Bhandari, P. & Gogate, P. 2018 Kinetic and thermodynamic study of adsorptive removal of sodium dodecyl benzene sulfonate using adsorbent based on thermo-chemical activation of coconut shell. *Journal of Molecular Liquids* **252**, 495–505.

Bhatnagar, A., Ji, M., Choi, Y., Jung, W., Lee, S., Kim, S., Lee, G., Suk, H., Kim, H., Min, B., Kim, S., Jeon, B. & Kang, J. 2008 Removal of nitrate from water by adsorption onto zinc chloride treated activated carbon. *Journal of Separation Science and Technology* **43**, 886–907.

Boopathy, R., Karthikeyan, S., Mandal, A. & Sekaran, G. 2012 Adsorption of ammonium ion by coconut shell-activated carbon from aqueous solution: kinetic, isotherm, and thermodynamic studies. *Journal of Environmental Science and Pollution Research* **20**, 533–542.

Cadaval, T. R. S., Guilherme, L. D. & Pinto, L. A. A. 2015 Equilibrium isotherms, thermodynamics, and kinetic studies for the adsorption of food azo dyes onto chitosan films. *Chemical Engineering Communications* **202**, 1316–1323.

Chan, O., Cheung, W. & McKay, G. 2011 Preparation and characterisation of demineralised tire derived activated carbon. *Journal of Carbon* **49**, 4674–4687.

Chen, H., Tu, Z., Wu, S., Yu, G., Du, C., Wang, H., Yang, E., Zhou, L., Deng, B., Wang, D. & Li, H. 2021 Recent advances in partial denitrification-anaerobic ammonium oxidation process for mainstream municipal wastewater treatment. *Chemosphere* **278**, 130436.

Cho, S., Kambey, C. & Nguyen, V. J. 2020 Performance of anammox processes for wastewater treatment: a critical review on effects of operational conditions and environmental stresses. *Journal of Water* **12**, 1–30.

Demiral, H. & Gündüzoğlu, G. J. 2010 Removal of nitrate from aqueous solutions by activated carbon prepared from sugar beet bagasse. *Journal of Bioresource Technology* **101**, 1675–1680.

Dong, Y., Yuan, H., Zhang, R. & Zhu, N. 2019 Removal of ammonia nitrogen from wastewater: a review. *American Society of Agricultural and Biological Engineers Journal* **62**, 1767–1778.

Fernandez, A., Barriocanal, C. & Alvarez, R. 2012 Pyrolysis of a waste from the grinding of scrap tyres. *Journal of Hazardous Materials* **203**, 236–243.

Gonçalves, M., Sánchez-García, L., Jardim, E., Silvestre-Albero, J. & Rodríguez-Reinoso, F. J. 2011 Ammonia removal using activated carbons: effect of the surface chemistry in dry and moist conditions. *Journal of Environmental Science and Technology* **45**, 10605–10610.

Hafshejani, L., Hooshmand, A., Naseri, A., Mohammadi, A., Abbasi, F. & Bhatnagar, A. 2016 Removal of nitrate from aqueous solution by modified sugarcane bagasse biochar. *Journal of Ecological Engineering* **95**, 101–111.

Hameed, B. & Daud, F. 2008 Adsorption studies of basic dye on activated carbon derived from agricultural waste: Hevea brasiliensis seed coat. *Chemical Engineering Journal* **139**, 48–55.

Kabuba, J. & Banza, M. 2021 Modification of clinoptilolite with dialkylphosphinic acid for the selective removal of cobalt (II) and nickel (II) from hydrometallurgical effluent. *Canadian Journal of Chemical Engineering* **99**, 168–178.

Kabuba, J., Lephallo, J. & Rutto, H. 2022 Comparison of various technologies used to eliminate nitrogen from wastewater: a review. *Journal of Water Process Engineering* **48**, 102885.

Kadhum, S. T., Alkindi, G. Y. & Albayati, T. M. 2021 Determination of chemical oxygen demand for phenolic compounds from oil refinery wastewater implementing different methods. *Desalination and Water Treatment* **231**, 44–53. doi:10.5004/dwt.2021.27443.

Karadag, D., Koc, K., Turan, M. & Armagan, B. 2006 Removal of ammonium ion from aqueous solution using natural Turkish clinoptilolite. *Journal of Hazardous Materials* **136**, 604–609.

Kotoulas, A., Agathou, D., Triantaphyllidou, I., Tatoulis, T., Akratos, C., Tekerlekopoulou, A. & Vayenas, D. 2019 Zeolite as a potential medium for ammonium recovery and second cheese whey treatment. *Journal of Water* **11**, 1–23.

López, F., Centeno, T., Rodríguez, O. & Alguacil, F. 2013 Preparation and characterization of activated carbon from the char produced in the thermolysis of granulated scrap tires. *Journal of the Air & Waste Management Association* **63**, 534–544.

Mazarji, M., Aminzadeh, B., Baghdadi, M. & Bhatnagar, A. 2017 Removal of nitrate from aqueous solution using modified granular activated carbon. *Journal of Molecular Liquids* **233**, 139–148.

Mohamed, W. S. & Abu-Dief, A. M. 2018 Synthesis, characterization and photocatalysis enhancement of Eu_2O_3-ZnO mixed oxide nanoparticles. *Journal of Physics and Chemistry of Solids* **116**, 375–385.

Mui, E., Cheung, W. & McKay, G. 2010 Tire char preparation from waste tire rubber for dye removal from effluents. *Journal of Hazardous Materials* **175**, 151–158.

Ren, Z., Jia, B., Zhang, G., Fu, X., Wang, Z., Wang, P. & Longyi, L. V. 2021 Study on adsorption of ammonia nitrogen by iron-loaded activated carbon from low temperature wastewater. *Journal of Chemosphere* **262**, 1–10.

Ruiz-Baltazar, A. J. 2018 Green composite based on silver nanoparticles supported on diatomaceous earth: kinetic adsorption models and antibacterial effect. *Journal of Cluster Science* **29**, 509–519.

Sabah, E., Turan, M. & Celik, M. 2002 Adsorption mechanism of cationic surfactants onto acid and heat-activated sepiolites. *Water Research Journal* **36**, 3957–3964.

Sastre, A., Martín, A. & Alonso, E. 2016 Adsorption of nickelocene and ruthenocene on mesoporous silica MCM-48 and activated carbon supports in supercritical carbon dioxide. *The Journal of Supercritical Fluids* **117**, 138–146.

Srivastava, S., Agrawal, S. B. & Mondal, M. K. 2016 Characterization, isotherm and kinetic study of Phaseolus vulgaris husk as an innovative adsorbent for Cr(VI) removal. *Korean Journal of Chemical Engineering* **33**, 567–575.

Suuberg, E. & Aarna, I. 2007 Porosity development in carbons derived from scrap automobile tires. *Journal of Carbon* **45**, 1719–1726.

Tanga, K., Zhanga, S., Rena, D., Zhanga, X., Zhanga, Z. & Zhanga, X. 2023 Study on the removal of Pb(II) from water by coated sulfur-modified nanoscale zero-valent iron. *Water Science & Technology*. https://doi.org/10.2166/wst.2023.053.

Vaičiukynienė, D., Mikelionienė, A., Baltušnikas, A., Kantautas, A. & Radzevičius, A. 2020 Removal of ammonium ion from aqueous solutions by using unmodifed and H_2O_2-modifed zeolitic waste. *Journal of Scientific Reports* **10**, 352–367.

Yang, H., Lou, K., Rajapaksha, A. & Ok, Y. 2018 Adsorption of ammonium in aqueous solutions by pine sawdust and wheat straw biochars. *Advances in Engineering Research Journal* **200**, 25638–25647.

Yian, Z., Yuntao, X. & Aiqin, W. 2012 Rapid and wide pH-independent ammonium-nitrogen removal using a composite hydrogel with three-dimensional networks. *Chemical Engineering Journal* **179**, 90–98.

Yorgun, S. & Yıldız, D. 2015 Preparation and characterization of activated carbons from Paulownia wood by chemical activation with H_3PO_4. *Journal of the Taiwan Institute of Chemical Engineers* **53**, 122–131.

First received 1 March 2023; accepted in revised form 10 May 2023. Available online 24 May 2023